

# SECOND HARMONICS EFFECTS IN RANDOM DUFFING OSCILLATORS \*

JUAN A. ACEBRÓN † AND RENATO SPIGLER ‡

*to George Papanicolaou on his 60th Birthday*

**Abstract.** We consider a stochastic model for Duffing oscillators, where the nonlinearity and the randomness are scaled in such a way that they interact strongly. A typical feature is the appearance of *second harmonics* effects. An asymptotic statistical analysis for these oscillators is performed in the *diffusion limit*, when a suitable *absorbing boundary* condition is imposed, according to the underlying physical problem. The related Fokker-Planck equation has been numerically solved to obtain the first two moments of the oscillator's displacement from its rest-position. Dependence on the nonlinearity strength and on the location of the absorbing boundary has also been investigated. Such results have been compared with those computed solving the corresponding stochastic Ito differential equations by a Monte Carlo method, where *quasi-random* sequences of numbers have been efficiently used.

**Key words.** nonlinear random oscillators, Duffing oscillators, Fokker-Planck equation, diffusions with absorbing boundaries, quasi-Monte Carlo methods.

**AMS subject classifications.** 34F05, 60H10, 60H35, 65C05

**1. Introduction.** Duffing oscillators are among the simplest types of *nonlinear* oscillators. They are governed by second-order ordinary differential equations, describing, e.g., the free motion that a particle performs around its rest-position, subject to a certain nonlinear restoring force. They have been extensively studied (see [25], e.g.). On the other hand, *random* harmonic (linear) oscillators have also been studied in the literature (see [13], e.g.).

In [23], a stochastic model for nonlinear oscillators of the Duffing-type has been considered, in order to investigate the joint effect of nonlinearity and randomness. However, these two mechanisms were scaled in such a way that the effect of the nonlinearity on the underlying linear random oscillator model turned out to be rather insignificant, in the long-time behavior. The topic of nonlinear random oscillators is still an active area of research, especially in connection with applications to engineering, see [5].

In this paper, a stochastic model for a Duffing-type oscillator is considered where the effect of the nonlinearity is much more important than that analyzed in [23]. The model equation is

$$(1.1) \quad y_\epsilon'' + 2\epsilon^2\lambda(t)y_\epsilon' + \omega_0^2 [1 + \epsilon\mu(t) + \epsilon w\nu(t)y_\epsilon^2] y_\epsilon = 0,$$

$$(1.2) \quad y_\epsilon(0) = y_1, \quad y_\epsilon'(0) = y_2,$$

where  $\epsilon$  represents a small real parameter,  $w$  is a real parameter which sizes the nonlinearity, and  $\lambda(\cdot)$ ,  $\mu(\cdot)$ ,  $\nu(\cdot)$  are suitable real-valued stochastic processes on some probability space. Therefore,  $y_\epsilon(\cdot)$  will be a (real-valued) stochastic process as well. An *absorbing condition* is further imposed to take into account that the representative

---

\* This work was carried out within the framework of the Italian GNFM-INdAM.

†Departamento de Automática, Escuela Politécnica, Universidad de Alcalá de Henares, Crta. Madrid-Barcelona, Km 31.600, 28871 Alcalá de Henares, Madrid, Spain ([juan.acebron@uah.es](mailto:juan.acebron@uah.es)),

‡Dipartimento di Matematica, Università di "Roma Tre", Largo S.L. Murialdo 1, 00146 Rome, Italy ([spigler@mat.uniroma3.it](mailto:spigler@mat.uniroma3.it)).

particle, whose random motion is described by Eq. (1.1), is lost whenever its position,  $y_\epsilon(t)$ , reaches a given value, say  $\pm R$ . This is the case of the so-called “accelerator problem”. In fact, when a beam of charged particles turns around in the vacuum, inside a toroidal chamber, whose cross section has radius  $R$ , confined by strong static magnetic fields, after a very large number of laps the beam opens up, and some particles are lost when they hit the material wall. We may think that here there is an absorbing boundary, and for a randomly perturbed problem this corresponds to a vanishing probability condition at a certain given radial distance from the center of the chamber. Clearly, such a condition amounts to imposing a boundary condition to the transition probability density obeying the Kolmogorov forward equation (Fokker-Planck). Therefore, the present problem subject to an absorbing boundary condition will be shown to possess a diffusion limit solution.

Note that only local existence and uniqueness of solutions to the problem (1.1)-(1.2) can be guaranteed. However, the absorbing boundary condition associated to such a problem allows for existence and uniqueness of solutions up to the first time when  $y_\epsilon(t)$  attains the value  $\pm R$  (for every fixed  $\epsilon$  and for every chosen realization of the noise terms). On the other hand, as soon as the considered trajectory ends up at the level  $\pm R$ , the corresponding particle is “killed” and goes out of the problem.

In [23], the nonlinear term  $\epsilon w \nu(t) y_\epsilon^2$  was replaced by the “weaker” one  $\epsilon^2 w \nu(\cdot) y_\epsilon^2$ , and the solution there was studied in the *diffusion limit*, attained when  $\epsilon \rightarrow 0$  on a suitably long time-scale. As it will be shown, the model described by (1.1)-(1.2) exhibits some different features with respect to that in [23]. Among the other things, stronger nonlinear effects, such as “second harmonics” effects can now be observed.

It can be seen that the present problem, without imposing the absorbing boundary condition above, does *not* possess a diffusion limit, since, according to the Feller-Hille theory [7, 9], the formally obtained Kolmogorov forward and backward equations do *not* have *unique* solutions. A comment on this problem is given in the last section.

In Section 2, the relevant assumptions on the stochastic processes  $\lambda(\cdot)$ ,  $\mu(\cdot)$ ,  $\nu(\cdot)$ , are made. A parabolic differential equation (the Fokker-Planck equation) is then derived, which describes the time evolution of the transition probability density of the limiting-process. Such a process approximates the process  $y_\epsilon$  in the diffusion limit. From this, the first two moments of the displacement of the oscillator are computed (Section 3). In Section 4, we describe the numerical treatment performed on such equation to get quantitative information. We also solved the underlying Itô stochastic differential equation, for the purpose of comparison. Such a simulation, which is of the Monte Carlo-type, has been accomplished by using quasi-random (low discrepancy) sequences of numbers [2, 3, 18]. This choice is alternative to that of the more common sequences of pseudorandom numbers, and here is shown to be effective due to the use of a “scrambling” strategy (a reordering technique [19]). This positive outcome contrasts with the earlier findings of [10], where the authors did not introduce any scrambling, see [1], however. Plots are given to illustrate the dependence of the moments on the various parameters, including the location  $R$  of the absorbing barrier, and the strength,  $w$ , of nonlinearity, and the results are discussed. In Section 5, the high points of the paper are summarized.

**2. Statistical analysis in the diffusion limit.** It is convenient to introduce the van der Pool coordinates,  $\rho_\epsilon$ ,  $\varphi_\epsilon$ , defined by

$$y_\epsilon(t) = \rho_\epsilon(t) \cos(\omega_0 t + \varphi_\epsilon(t)), \quad y'_\epsilon(t) = -\omega_0 \rho_\epsilon(t) \sin(\omega_0 t + \varphi_\epsilon(t)).$$

Note that  $\rho_\epsilon^2 = y_\epsilon^2 + \omega_0^{-2} y_\epsilon'^2$  represents the energy of the oscillator. By using this transformation in (1.1)-(1.2), the system

$$(2.1) \quad \frac{d}{dt} \begin{pmatrix} \rho_\epsilon \\ \varphi_\epsilon \end{pmatrix} = \epsilon \begin{pmatrix} F_1 \\ F_2 \end{pmatrix} + \epsilon^2 \begin{pmatrix} G_1 \\ G_2 \end{pmatrix},$$

where  $F_i \equiv F_i(t, \rho_\epsilon, \varphi_\epsilon)$ ,  $G_i \equiv G_i(t, \rho_\epsilon, \varphi_\epsilon)$ , is obtained along with the initial conditions

$$(2.2) \quad \rho_\epsilon(0) = (y_1^2 + y_2^2/\omega_0^2)^{1/2}, \quad \varphi_\epsilon(0) = -\arctan(y_2/\omega_0 y_1)^{1/2},$$

where we set, for short,

$$F_1 := \frac{\omega_0}{2} \rho_\epsilon \left\{ \mu(t) \sin(2\omega_0 t + 2\varphi_\epsilon) + \nu(t) \frac{w}{2} \rho_\epsilon^2 [1 + \cos(2\omega_0 t + 2\varphi_\epsilon)] \sin(2\omega_0 t + 2\varphi_\epsilon) \right\},$$

$$(2.3) \quad F_2 := \frac{\omega_0}{2} \left\{ \mu(t) [1 + \cos(2\omega_0 t + 2\varphi_\epsilon)] + \nu(t) \frac{w}{2} \rho_\epsilon^2 [1 + \cos(2\omega_0 t + \varphi_\epsilon)]^2 \right\},$$

$$G_1 := -\rho_\epsilon \lambda(t) [1 - \cos(2\omega_0 t + 2\varphi_\epsilon)],$$

$$G_2 := -\lambda(t) \sin(2\omega_0 t + 2\varphi_\epsilon).$$

Below, we shall assume that  $\lambda(\cdot)$ ,  $\mu(\cdot)$ , and  $\nu(\cdot)$  are real-valued, almost-surely bounded, wide-sense stationary stochastic processes, on some probability space,  $(\Omega, \mathcal{A}, P)$ . The dependence on the chance will be omitted throughout, as is customary. We shall assume that

$$(2.4) \quad E[\lambda(t)] = \lambda_0, \quad E[\mu(t)] = 0, \quad E[\nu(t)] = 0,$$

for some constant  $\lambda_0$ , where  $E[\cdot]$  denotes taking expected values. Moreover, we shall assume that  $\mu(\cdot)$  and  $\nu(\cdot)$  satisfy a *mixing* condition, in a sufficiently *strong* sense (see [20, 21], e.g.). As for the stationarity, we shall assume below that  $\mu(\cdot)$  and  $\nu(\cdot)$  are stationarily correlated (see [4], p. 160; [26], pp. 78-79), with covariance matrix

$$(2.5) \quad \begin{pmatrix} E[\mu(s)\mu(\sigma)] & E[\mu(s)\nu(\sigma)] \\ E[\nu(s)\mu(\sigma)] & E[\nu(s)\nu(\sigma)] \end{pmatrix},$$

whose entries will be denoted by  $R_{ij}(s - \sigma)$ ,  $i, j = 1, 2$ .

Under these hypotheses, we want to investigate whether the process converges weakly to some limiting-process when  $\epsilon \rightarrow 0$  and  $t \rightarrow +\infty$ , with  $\tau := \epsilon^2 t = \text{const.}$ , uniformly on  $0 \leq \tau \leq \tau_0$  (diffusion limit). Indeed, under similar hypotheses, this was proved to be true for the Duffing model studied in [23]. In that case, the limiting-process, denoted by  $(\rho(\tau), \varphi(\tau))$ , turned out to be a Markov process with trajectories continuous with probability 1. Therefore, it could be described by its infinitesimal generator

$$(2.6) \quad L := \sum_{i,j=1}^2 a_{ij}(z) \frac{\partial^2}{\partial z_i \partial z_j} + \sum_{i=1}^2 [b_i(z) + c_i(z)] \frac{\partial}{\partial z_i},$$

where we set  $z := (z_1, z_2)^T$  ( $z_1 = \rho$ ,  $z_2 = \varphi$ , for us), and  $a_{ij}$ ,  $b_i$ ,  $c_i$  are given by

$$a_{ij}(z) := \lim_{t \rightarrow +\infty} \frac{1}{t} \int_0^t \int_0^s E [F_i(s, z) F_j(\sigma, z)] ds d\sigma, \quad i, j = 1, 2,$$

$$(2.7) \quad b_i(z) := \lim_{t \rightarrow +\infty} \frac{1}{t} \int_0^t \int_0^s \sum_{j=1}^2 E \left[ \frac{\partial F_i(s, z)}{\partial z_j} F_j(\sigma, z) \right] ds d\sigma, \quad i = 1, 2,$$

$$c_i(z) := \lim_{t \rightarrow +\infty} \frac{1}{t} \int_0^t E [G_i(s, z)] ds, \quad i = 1, 2.$$

Here, we can proceed similarly, taking as quantities  $F_i, G_i$ ,  $i = 1, 2$ , those appearing here are those defined in (2.3). This theorem is of the type of Khasminskii's [12] (see also [24]), as used in [20, 21].

In our problem, it is possible to evaluate explicitly the quantities in (2.7). Though this is an elementary task, the derivation is quite lengthy, see [23], e.g.. Therefore, we skip the details and give only the results (obtained using the assumptions on  $\lambda(\cdot)$ ,  $\mu(\cdot)$ ,  $\nu(\cdot)$ ):

$$a_{11}(\rho) = \rho^2 \left[ \beta_{11}(2) + \frac{w}{2} \rho^2 (\beta_{12}(2) + \beta_{21}(2)) + \frac{w^2}{4} \rho^4 (\beta_{22}(2) + \frac{1}{4} \beta_{22}(4)) \right],$$

$$a_{12}(\rho) + a_{21}(\rho) = \frac{w}{2} \rho^3 (\gamma_{12}(2) - \gamma_{21}(2)),$$

$$a_{22}(\rho) = 2\alpha_{11} + \beta_{11}(2) + \frac{w}{2} \rho^2 [3(\alpha_{12} + \alpha_{21}) + 2(\beta_{12}(2) + \beta_{21}(2))]$$

$$(2.8) \quad + \frac{w^2}{16} \rho^4 (18\alpha_{22} + 16\beta_{22}(2) + \beta_{22}(4)),$$

$$b_1(\rho) = \rho \left[ 3\beta_{11}(2) + \frac{5}{2} w \rho^2 (\beta_{12}(2) + \beta_{21}(2)) + \frac{7}{16} w^2 \rho^4 (4\beta_{22}(2) + \beta_{22}(4)) \right],$$

$$b_2(\rho) = 2 \left[ \gamma_{11}(2) + w \rho^2 (2\gamma_{12}(2) + \gamma_{21}(2)) + \frac{3}{2} w^2 \rho^4 (\gamma_{22}(2) + \frac{1}{8} \gamma_{22}(4)) \right],$$

$$c_1(\rho) = -\lambda_0 \rho, \quad c_2(\rho) = 0,$$

where the notation

$$\alpha_{ij} := \frac{\omega_0^2}{8} \int_0^{+\infty} R_{ij}(x) dx,$$

$$(2.9) \quad \beta_{ij}(k) := \frac{\omega_0^2}{8} \int_0^{+\infty} R_{ij}(x) \cos(k\omega_0 x) dx, \quad k = 2, 4,$$

$$\gamma_{ij}(k) := \frac{\omega_0^2}{8} \int_0^{+\infty} R_{ij}(x) \sin(k\omega_0 x) dx, \quad k = 2, 4,$$

has been used.

**Remark 2.1.** Note that  $a_{ij}$ ,  $b_i$ ,  $c_i$  depend only on  $\rho$  (and not on  $\varphi$ ).

**Remark 2.2.** Observe that in this model there is an effect due to the 2nd harmonics, through the terms  $\beta_{22}(4)$ ,  $\gamma_{22}(4)$ .

**Remark 2.3.** In the model studied in [23],  $\nu(\cdot)$  had to be “strong enough”, in order to be effective, because the nonlinearity was weak (of order  $\mathcal{O}(\epsilon^2)$ ) in comparison to the randomness (of order  $\mathcal{O}(\epsilon)$ ). For example,  $E[\nu(\cdot)] \notin L(\mathbf{R}^+)$ ;  $\nu(t) = \text{const.} \neq 0$  was acceptable. However,  $E[\nu(\cdot)]$  had to be constant (0 or not), by the assumed stationarity.

In the present model, in some sense,  $\nu(\cdot)$  has to be “not too strong”, because the nonlinearity term now is considerably more important: A finite second moment, with a correlation function decaying to zero sufficiently fast, is required (by the mixing property), and  $E[\nu(\cdot)] \equiv 0$  by the stationarity.

With the infinitesimal generator given by (2.6), (2.8), we can write down the Kolmogorov forward (or Fokker-Planck) equation

$$(2.10) \quad \frac{\partial p}{\partial \tau} = L^*[p],$$

$\tau := \epsilon^2 t$ , satisfied by the transition probability density  $p$ ,  $L^*$  denoting the adjoint operator of  $L$  (defined in (2.6)-(2.7)). Such equation should be considered along with the initial value (IV)

$$(2.11) \quad p(\rho, \varphi; 0) = \delta(\rho - \rho_0) \delta(\varphi - \varphi_0),$$

where  $\rho_0$  and  $\varphi_0$  are the initial values of  $\rho(t)$  and  $\varphi(t)$ , and the boundary condition (BC)

$$(2.12) \quad p(R, \varphi, \tau) = 0,$$

correspondingly to the absorbing boundary located at  $\rho = R$ .

We can then evaluate, in particular, the *moments* of the limiting-process  $y(\tau) := \rho(\tau) \cos(\omega_0 t + \varphi(\tau))$ . It is convenient to write (2.10) in the form

$$(2.13) \quad \begin{aligned} \frac{\partial p}{\partial \tau_1} &= \frac{\partial^2}{\partial \rho^2} [(1 + A_1 w \rho^2 + A_2 w^2 \rho^4) \rho^2 p] + \frac{\partial^2}{\partial \rho \partial \varphi} (B_1 w \rho^3 p) \\ &+ \frac{\partial^2}{\partial \varphi^2} [(C_0 + C_1 w \rho^2 + C_2 w^2 \rho^4) p] - \frac{\partial}{\partial \rho} [(D_0 + D_1 w \rho^2 + D_2 w^2 \rho^4) \rho p] \\ &- \frac{\partial}{\partial \varphi} [(E_0 + E_1 w \rho^2 + E_2 w^2 \rho^4) p], \end{aligned}$$

where

$$(2.14) \quad \tau_1 := \beta_{11}(2) \tau \equiv \beta_{11}(2) \epsilon^2 t,$$

$$\begin{aligned}
A_1 &:= \frac{\beta_{12}(2) + \beta_{21}(2)}{2\beta_{11}(2)}, \\
A_2 &:= \frac{\beta_{22}(2) + \frac{1}{4}\beta_{22}(4)}{4\beta_{11}(2)}, \\
B_1 &:= \frac{\gamma_{12}(2) - \gamma_{21}(2)}{2\beta_{11}(2)}, \\
C_0 &:= 2\frac{\alpha_{11}}{\beta_{11}(2)} + 1, \\
C_1 &:= \frac{3(\alpha_{12} + \alpha_{21}) + 2(\beta_{12}(2) + \beta_{21}(2))}{2\beta_{11}(2)}, \\
C_2 &:= \frac{18\alpha_{22} + 16\beta_{22}(2) + \beta_{22}(4)}{16\beta_{11}(2)}, \\
D_0 &:= 3 - \frac{\lambda_0}{\beta_{11}(2)}, \\
D_1 &:= \frac{5(\beta_{12}(2) + \beta_{21}(2))}{2\beta_{11}(2)} \equiv 5A_1, \\
D_2 &:= \frac{7(\beta_{22}(2) + \frac{1}{4}\beta_{22}(4))}{4\beta_{11}(2)} \equiv 7A_2, \\
E_0 &:= 2\frac{\gamma_{11}(2)}{\beta_{11}(2)}, \\
E_1 &:= \frac{2(2\gamma_{12}(2) + \gamma_{21}(2))}{\beta_{11}(2)}, \\
E_2 &:= \frac{3(\gamma_{22}(2) + \frac{1}{8}\gamma_{22}(4))}{2\beta_{11}(2)}.
\end{aligned}
\tag{2.15}$$

Note the presence of some “second harmonics” terms (see Remark 2.2), which enter the coefficients above via the quantities  $\beta_{22}(4)$ ,  $\gamma_{22}(4)$ . Their effect is to increase the value of  $A_2$ ,  $C_2$ ,  $D_2$ , and  $E_2$ , and thus, qualitatively, to increase the nonlinearity size, as  $|w|$  would have been increased. Moreover, this happens independently of the sign of  $w$ .

**Remark 2.4.** It is worth noting that the solution to problem (2.10)-(2.12) is not ( $L^1$ ) norm-increasing. In fact, integrating both sides of equation (2.13) on the domain  $[0, 2\pi] \times [0, R]$ , obtains

$$\begin{aligned}
&\frac{\partial}{\partial \tau_1} \int_0^{2\pi} \int_0^R p(\rho, \varphi, \tau_1) d\rho d\varphi \\
(2.16) \quad &= R^2(1 + A_1 w R^2 + A_2 w^2 R^2) \int_0^{2\pi} \frac{\partial p}{\partial \rho}(R, \varphi, \tau_1) d\varphi
\end{aligned}$$

where the absorbing boundary condition in (2.12) has been used. We now observe that  $\partial p(R, \varphi, \tau_1)/\partial \rho \leq 0$ . In fact, such a quantity is nonpositive being  $p$  positive inside the domain, and zero on the boundary  $\rho = R$ . Therefore,  $dP(\tau_1)/d\tau_1 \leq 0$ , where

$$(2.17) \quad P(\tau_1) := \int_0^{2\pi} \int_0^R p(\rho, \varphi, \tau_1) d\rho d\varphi.$$

The quantity  $P(\tau_1)$  represents the *survival probability* of the particle up to time  $\tau_1$ , that is the probability that the particle does not hit the absorbing barrier before time

$\tau_1$ . A similar result can be found in [6], where it is shown that, in presence of an absorbing boundary condition, the norm of any initial data is not preserved.

In the special but important case that  $\mu(\cdot)$  and  $\nu(\cdot)$  are *uncorrelated* (possibly independent), there are some simplifications. As  $R_{12}(\cdot) \equiv R_{21}(\cdot) \equiv 0$  in this case, the partial differential equation in (2.10) reduces to

$$(2.18) \quad \frac{\partial p}{\partial \tau_1} = \frac{\partial^2}{\partial \rho^2} [(1 + A_2 w^2 \rho^4) \rho^2 p] + \frac{\partial^2}{\partial \varphi^2} [(C_0 + C_2 w^2 \rho^4) p] \\ - \frac{\partial}{\partial \rho} [(D_0 + D_2 w^2 \rho^4) \rho p] - \frac{\partial}{\partial \varphi} [(E_0 + E_2 w^2 \rho^4) p].$$

Note that now the coefficients of the equation depend only on  $w^2$ , and therefore the results are *independent of the sign* of  $w$ . This is not true when  $\mu(\cdot)$  and  $\nu(\cdot)$  are correlated. Note also that the effects of the second harmonics only depends on the autocorrelation of  $\nu(\cdot)$ ,  $R_{22}(\cdot)$  (in  $A_2, C_2, D_2, E_2$ , such an effect enters through  $\beta(4)$  and  $\gamma(4)$ ).

**3. The time evolution of the moments.** As the equation in (2.13) is linear and has coefficients independent of  $\varphi$ , we can Fourier analyze it. Expanding  $p$  in Fourier series,

$$p(\rho, \varphi, \tau_1) = \sum_{m=-\infty}^{+\infty} p_m(\rho, \tau_1) e^{i m \varphi},$$

we obtain for the  $m$ th coefficient

$$(3.1) \quad p_m(\rho, \tau_1) = \frac{1}{2\pi} \int_0^{2\pi} p(\rho, \varphi, \tau_1) e^{-i m \varphi} d\varphi$$

the evolution equation

$$(3.2) \quad \frac{\partial p_m}{\partial \tau_1} = \frac{\partial^2}{\partial \rho^2} [(1 + A_1 w \rho^2 + A_2 w^2 \rho^4) \rho^2 p_m] \\ - \frac{\partial}{\partial \rho} [(D_0 + (D_1 + i m B_1) w \rho^2 + D_2 w^2 \rho^4) \rho p_m] \\ + i m [(i m C_0 - E_0) + (i m C_1 - E_1) w \rho^2 + (i m C_2 - E_2) w^2 \rho^4] p_m,$$

with the IV,

$$(3.3) \quad p_m(\rho, 0) = \frac{1}{2\pi} \delta(\rho - \rho_0) e^{-i m \varphi_0},$$

and the BC

$$(3.4) \quad p_m(R, \tau_1) = 0.$$

The boundary point  $\rho = R$  is a *regular* boundary, while  $\rho = 0$  is a *natural boundary*, according to the Feller's classification (see [7, 9]). On a natural boundary,

such as  $\rho = 0$ , no BC is required, while a condition is needed on a regular boundary in order that the Fokker-Planck equation has a unique solution. In [7], Sec. 23, the boundary value problem for the one dimensional diffusion equation

$$(3.5) \quad u_t = \frac{\partial^2}{\partial x^2}(a(x)u) - \frac{\partial}{\partial x}(b(x)u),$$

and its adjoint has been considered on the interval  $-\infty \leq r_1 < x < r_2 \leq +\infty$ . Depending on the nature of the boundary points,  $r_1, r_2$ , and the type of data imposed on them to the solution, such equations may have or may not have a unique solution. Defining the function

$$(3.6) \quad W(x) := \exp \left\{ - \int_{x_0}^x \frac{b(s)}{a(s)} ds \right\},$$

where  $x_0 \in (r_1, r_2)$ , the boundary points were classified as follows:

- the boundary  $r_j$  is *regular* if  $W(x) \in L^1(x_0, r_j)$  and  $a^{-1}(x)W^{-1}(x) \in L^1(x_0, r_j)$ ;
- it is an *exit* boundary if  $a^{-1}(x)W^{-1}(x) \notin L^1(x_0, r_j)$ , and  $W(x) \int_{x_0}^x a^{-1}(s)W^{-1}(s) ds \in L^1(x_0, r_j)$ ;
- it is an *entrance* boundary if  $a^{-1}(x)W^{-1}(x) \in L^1(x_0, r_j)$ , and  $a^{-1}(x)W^{-1}(x) \int_{x_0}^x W(s) ds \in L^1(x_0, r_j)$ ;
- it is *natural* in all other cases.

One may observe that for the heat equation,  $u_t = u_{xx}$ , the boundaries  $r_j = \pm\infty$  are both natural, while they are regular when they are finite.

It is straightforward to check that for our problem in equation (3.2),  $r_1 = \rho = 0$  is a natural boundary, while  $r_2 = \rho = R$  is a regular boundary. It follows from Feller's theory that our problem possesses a unique solution when the absorbing boundary condition in (3.4) is prescribed, while no condition is imposed on  $\rho = 0$ .

In the special case of  $\mu(\cdot), \nu(\cdot)$  uncorrelated, equation (2.13) reduces to (2.18) and we get the simpler problem

$$(3.7) \quad \begin{aligned} \frac{\partial p_m}{\partial \tau_1} &= \frac{\partial^2}{\partial \rho^2} [(1 + A_2 w^2 \rho^4) \rho^2 p_m] + \frac{\partial}{\partial \rho} [(D_0 + D_2 w^2 \rho^4) \rho p_m] \\ &\quad + im [(imC_0 - E_0) + (imC_2 - E_2) w^2 \rho^4] p_m, \\ p_m(\rho, 0) &= \frac{1}{2\pi} \delta(\rho - \rho_0) e^{-im\varphi_0}, \quad p_m(R, \tau_1) = 0. \end{aligned}$$

We are primarily interested in computing the first two moments of the displacement  $y_\epsilon(\cdot)$  of the oscillator, by approximating it with the limiting-process  $y(\cdot)$ . For this we have

$$(3.8) \quad E_{\rho_0, \varphi_0}[y(\tau)] = \text{Re} \left\{ e^{i\omega_0 t} E_{\rho_0, \varphi_0}[\rho(\tau) e^{i\varphi(\tau)}] \right\},$$

$$E_{\rho_0, \varphi_0}[y^2(\tau)] = \frac{1}{2} E_{\rho_0, \varphi_0}[\rho^2(\tau)] + \frac{1}{2} \text{Re} \left\{ e^{2i\omega_0 t} E_{\rho_0, \varphi_0}[\rho^2(\tau) e^{2i\varphi(\tau)}] \right\},$$

where the quantities  $E_{\rho_0, \varphi_0}[\rho^k(\tau) e^{ik\varphi(\tau)}]$ ,  $k = 1, 2$ , and  $E_{\rho_0, \varphi_0}[\rho^2(\tau)]$  can be computed integrating (3.1) [or (3.7)]. Recall that  $\tau_1 = \beta_{11}(2)\epsilon^2 t$ , see (2.14). We obtain

$$(3.9) \quad E_{\rho_0, \varphi_0}[y(\tau_1)] = 2\pi \text{Re} \left[ \int_0^R \rho p_1(\rho, \tau_1) d\rho \right] \cos \omega_0 t + 2\pi \text{Im} \left[ \int_0^R \rho p_1(\rho, \tau_1) d\rho \right] \sin \omega_0 t,$$



$$(3.10) \quad E_{\rho_0, \varphi_0}[y^2(\tau_1)] = \pi \int_0^R \rho^2 p_0(\rho, \tau_1) d\rho + \pi \left\{ \text{Re} \left[ \int_0^R \rho^2 p_2(\rho, \tau_1) d\rho \right] \cos(2\omega_0 t) + \text{Im} \left[ \int_0^R \rho^2 p_2(\rho, \tau_1) d\rho \right] \sin(2\omega_0 t) \right\}.$$

The problem is clearly affected by *two time scales*, the fast (deterministic) scale, according to the “time”  $\omega_0 t$ , and the slow scale  $\tau_1$  on which nontrivial random phenomena occur in the diffusion limit, see [23]. In fact, it is over long times that the statistical cumulative effect of the small size noise becomes significant.

In the next section, we shall describe the numerical treatment carried out to solve the aforementioned problems. We shall give the relevant results in the form of several plots, and discuss the observed features.

**4. Numerical treatment.** We solved numerically problem (3.7) for  $m = 0, 1, 2$  on  $(0, R) \times (0, T)$ , with the BC in (2.12), obtaining the Fourier coefficients,  $p_m(\rho, \tau_1)$ , of the transition probability density,  $p(\rho, \varphi, \tau_1)$ . The covariance matrix  $\{R_{ij}(\cdot)\}_{i,j=1,2}$  had also to be specified. In the case above, where  $\mu(\cdot)$ ,  $\nu(\cdot)$  are supposed to be uncorrelated, we have only to assign  $R_{11}(\cdot)$  and  $R_{22}(\cdot)$ . Let choose

$$(4.1) \quad R_{11}(t) := e^{-\sigma_1 |t|}, \quad R_{22}(t) := e^{-\sigma_2 |t|},$$

for some positive constants  $\sigma_1, \sigma_2$ . Then all quantities  $\alpha_{ij}$ ,  $\beta_{ij}$ ,  $\gamma_{ij}$ , and hence  $A_2$ ,  $D_0$ ,  $D_2$ ,  $C_0$ ,  $C_2$ ,  $E_0$  and  $E_2$ , can be computed.

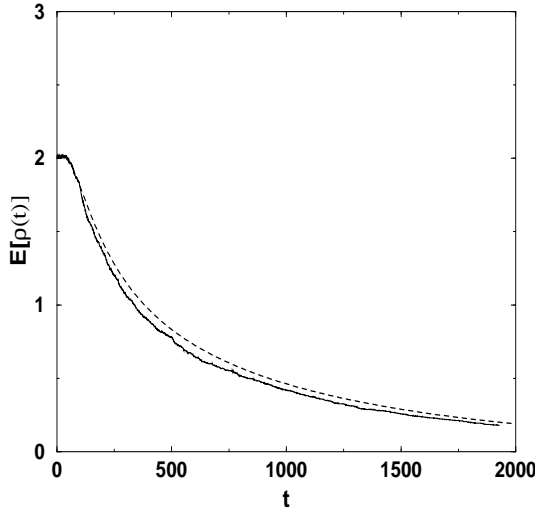


FIG. 4.1. Time evolution of the expected value of  $\rho$ . The nonlinearity size is  $w = 0.3$ . The dashed line represents the solution obtained through the Fokker-Planck equation; the continuous line is obtained solving the stochastic differential equation. The other parameters are  $\epsilon = 0.1$ ,  $\sigma_2/\sigma_1 = 1$ ,  $\omega_0/\sigma_1 = 1$ , and  $\lambda_0/\omega_0 = 3\beta_{11}(2)/2$ .

To be more explicit, we get from (2.9)

$$(4.2) \quad \alpha_{ii} = \frac{\omega_0^2}{8} \frac{1}{\sigma_i}, \quad \beta_{ii}(q) = \frac{\omega_0^2}{8} \frac{\sigma_i}{\sigma_i^2 + q^2 \omega_0^2}, \quad \gamma_{ii}(q) = \frac{\omega_0^2}{8} \frac{q \omega_0}{\sigma_i^2 + q^2 \omega_0^2}, \quad i = 1, 2,$$

and therefore from (2.15)

$$(4.3) \quad A_2 = \frac{1}{4} \frac{\sigma_2}{\sigma_1} \left( 1 + \frac{4\omega_0^2}{\sigma_1^2} \right) \left[ \frac{1}{\sigma_2^2/\sigma_1^2 + 4\omega_0^2/\sigma_1^2} + \frac{1/4}{\sigma_2^2/\sigma_1^2 + 16\omega_0^2/\sigma_1^2} \right],$$

$$(4.4) \quad D_0 = 3 - 8 \frac{\lambda_0/\omega_0}{\omega_0/\sigma_1} \left( 1 + 4 \frac{\omega_0^2}{\sigma_1^2} \right),$$

$$(4.5) \quad D_2 = 7A_2,$$

$$(4.6) \quad C_0 = 3 + 8 \frac{\omega_0^2}{\sigma_1^2},$$

$$(4.7) \quad C_2 = \frac{9}{8} \frac{1 + 4\omega_0^2/\sigma_1^2}{\sigma_2/\sigma_1} + \frac{\sigma_2}{\sigma_1} \frac{1 + 4\omega_0^2/\sigma_1^2}{\sigma_2^2/\sigma_1^2 + 4\omega_0^2/\sigma_1^2} + \frac{1}{16} \frac{\sigma_2}{\sigma_1} \frac{1 + 4\omega_0^2/\sigma_1^2}{\sigma_2^2/\sigma_1^2 + 16\omega_0^2/\sigma_1^2},$$

$$(4.8) \quad E_0 = 4 \frac{\omega_0}{\sigma_1},$$

$$(4.9) \quad E_2 = \frac{3}{2} \left[ 2 \frac{\omega_0}{\sigma_1} \frac{1 + 4\omega_0^2/\sigma_1^2}{\sigma_2^2/\sigma_1^2 + 4\omega_0^2/\sigma_1^2} + \frac{1}{2} \frac{\omega_0}{\sigma_1} \frac{1 + 4\omega_0^2/\sigma_1^2}{\sigma_2^2/\sigma_1^2 + 16\omega_0^2/\sigma_1^2} \right].$$

These expressions make it clear that only the *nondimensional* quantities

$$(4.10) \quad \frac{\sigma_2}{\sigma_1}, \quad \frac{\omega_0}{\sigma_1}, \quad \text{and} \quad \frac{\lambda_0}{\omega_0}$$

play a role and therefore need to be assigned. Another parameter is the ratio of the *two time scales*, which characterize the deterministic oscillations *and* the random fluctuations. We have from (2.14) and (4.2)

$$(4.11) \quad \tau_1 \equiv \beta_{11}(2)\epsilon^2 t = \frac{\epsilon^2}{8} \frac{\omega_0/\sigma_1}{1 + 4\omega_0^2/\sigma_1^2} \omega_0 t =: \kappa \omega_0 t$$

(note that  $\tau_1$  is nondimensional), and, for  $\omega_0/\sigma_1 \approx 1$ ,  $\epsilon \approx 0.1$ , we get  $\kappa \approx 4000$ . Note that  $\kappa$  is automatically determined by choosing  $\epsilon$  and  $\omega_0/\sigma_1$ . Therefore, we can assign  $\kappa$  or  $\epsilon$ , besides the previous parameters.

The numerical treatment consists of implementing an *implicit* scheme of finite-differences, with forward time-differences and space-centered differences (the Crank-Nicholson scheme). We chose  $R = 4$  and divided  $[0, R]$  in sections of equal length  $\Delta\rho = 10^{-3}$ ; the time-step size we used was  $\Delta\tau_1 = 10^{-4}$ , and the initial position of the oscillator was  $\rho_0 = 2$ . The parameters  $w$  and  $\lambda_0/\omega_0$  were varied to form several combinations, in order to investigate the various effects, while we kept  $\epsilon$  to the fixed value  $\epsilon = 0.1$ . The case  $\epsilon = 0.5$  was also considered to test the validity of the limiting theory. The first two moments

$$(4.12) \quad E[\rho^k(\tau_1)] = 2\pi \int_0^R \rho^k p_0(\rho, \tau_1) d\rho, \quad k = 1, 2,$$

of the oscillator's amplitude,  $\rho(\tau_1)$ , defined by the van der Pool variables (in the diffusion limit) can then be evaluated. Note that  $E[\rho^0] = E[1]$  coincides with the survival probability given by (2.17).

In Fig. 4.1, we plotted  $E[\rho]$  versus  $t$  for  $w = 0.3$ ,  $\sigma_2/\sigma_1 = 1$ ,  $\omega_0/\sigma_1 = 1$ , and  $\lambda_0/\omega_0 = 3\beta_{11}(2)/2$ . In Fig. 4.2, the time evolution of the second moment  $E[\rho^2]$  is shown for the same set of parameters. Recall that  $\rho_\epsilon^2 = y_\epsilon^2 + \omega_0^{-2} y_\epsilon'^2$  represents the energy of the oscillator governed by (1.1), and hence  $E[\rho^2]$  is the average energy of

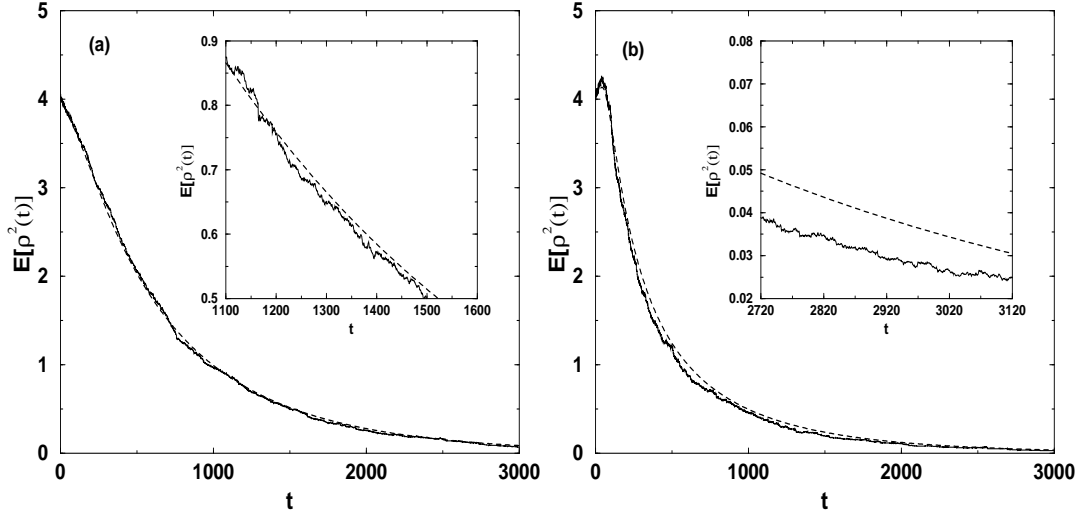


FIG. 4.2. Time evolution of the expected value of  $\rho^2$  for two different values of the nonlinearity parameter: (a)  $w = 0$ , and (b)  $w = 0.3$ . The other parameters are as in Fig. 4.1. A magnification of part of the plot is shown in the inset.

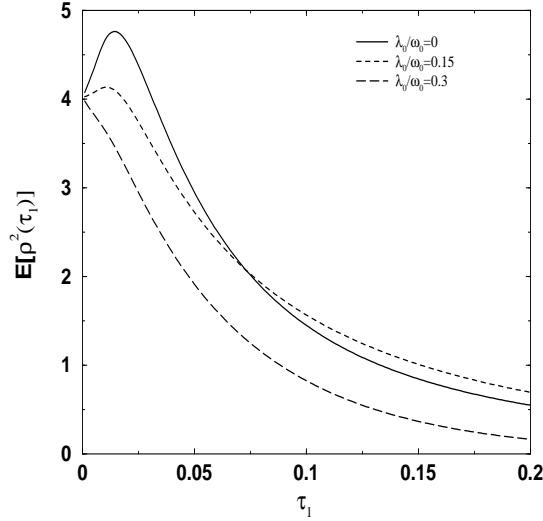


FIG. 4.3. Time evolution of the expected value of  $\rho^2$  for three different values of  $\lambda_0/\omega_0$ , keeping  $w$  to the fixed value 0.3. The other parameters are as in Fig. 4.1.

the oscillator in the diffusion limit. Here we also plotted  $E[\rho^2]$  for  $w = 0$ , that is for the corresponding linear harmonic oscillator, for the purpose of comparison.

In Fig. 4.3, we plotted  $E[\rho^2]$  versus  $\tau_1$  for the same values of the parameters used above, except that we considered several values of  $\lambda_0/\omega_0$ . It is apparent that there is “a threshold” when  $\lambda_0/\omega_0$  goes across a certain value. Above such a value (that is when the damping is sufficiently strong),  $E[\rho^2]$  decreases monotonically in time. Below the threshold value, initially  $E[\rho^2]$  grows in time undergoing a kind of transient behavior, but then it decays in order to match the absorbing boundary

condition. Such threshold is determined by the sign of the coefficient  $D_0$  which takes the values 3,  $-3$ ,  $-9$  correspondingly to the values  $\lambda_0/\omega_0 = 0, 0.15, 0.3$ , respectively.

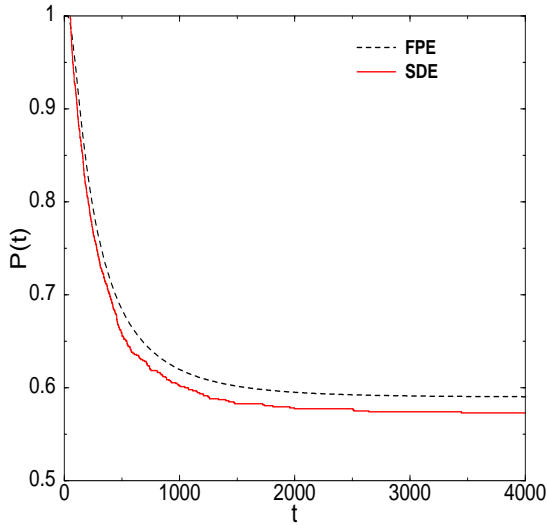


FIG. 4.4. Time evolution of the survival probability  $P(t)$  keeping  $w$  to the fixed value 0.3 and  $\lambda_0/\omega_0 = 0.15$ . The other parameters are as in Fig. 4.1.

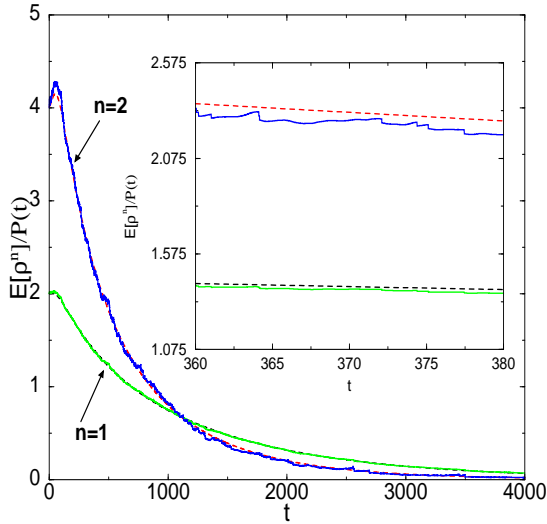


FIG. 4.5. Time evolution of two conditional moments of  $\rho$  with  $n = 1, 2$ . The parameters are as in Fig. 4.4.

Figure 4.4 shows the time evolution of the survival probability  $P(t)$  given by (2.17). This has been computed from both, the Fokker-Planck equation and by Monte Carlo simulations to provide a mutual validation. The time evolution of two conditional moments of  $\rho$ , assuming that the time  $\tau_1$  is less than the first hitting time, say  $\tau_R$ , is plotted in Fig. 4.5. Such moments can be obtained knowing the moments  $E[\rho^k]$

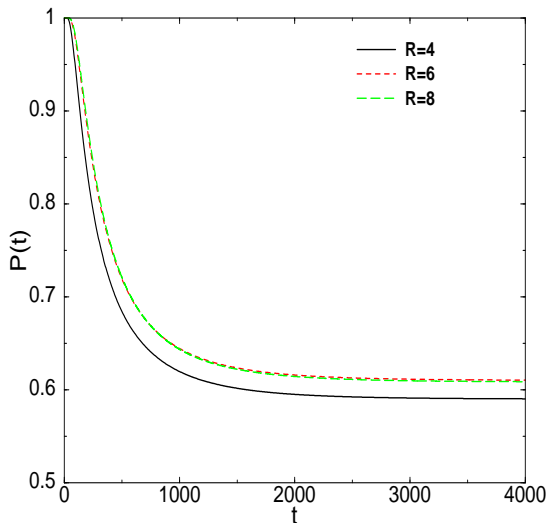


FIG. 4.6. Time evolution of the survival probability  $P(t)$  for three different values of  $R$ , obtained solving the Fokker-Planck equation. The parameters are as in Fig. 4.4.

and the survival probability  $P(\tau_1)$  as follows:

$$(4.13) \quad E[\rho^k | \tau_1 < \tau_R] = \frac{E[\rho^k(\tau_1)]}{P(\tau_1)}.$$

These quantities have been computed from the Fokker-Planck equation. The same quantities have been obtained from the corresponding stochastic differential equations by Monte Carlo simulations, for the purpose of validation, and plotted in Fig. 4.5 (solid line).

It is worth noting that the survival probability seems to stabilize around a nonzero value, and the conditional moments of  $\rho$  goes to zero, when time is sufficiently large. From both such features, the behavior of the surviving particles for long time can be easily understood. The nonzero value of  $P(t)$ , say  $p_\infty$ , would mean that a certain number of particles never exits from the boundary, while being zero the limiting value of the conditional moments when time goes to infinity, indicates that the surviving particles will be located with high probability around  $\rho = 0$ .

In Fig. 4.6, the time evolution of the survival probability,  $P(t)$ , is plotted for three different values of  $R$ . Recall that the parameter  $R$  is part of the data of the problem. For instance, in the example of the particle accelerator,  $R$  may be the radius of a vacuum chamber. Note that increasing the value of  $R$  makes larger the stationary value of  $P(t)$ . Clearly, when the boundary  $R$  is closer to the initial value  $\rho = \rho_0$ , the exiting probability of a given particle becomes larger, thus making the survival probability smaller in this case. Nevertheless, for sufficiently large values of  $R$ , such a probability seems to become independent of  $R$ . However, larger values of  $R$  cannot be used in practice, to prevent computational overflow, in view of the exponential dependence of some coefficients in the Fokker-Planck equation.

In Fig. 4.7, the survival probability has been plotted as function of time for two pairs of values of the nonlinearity parameter,  $w$ , and of the location of the absorbing barrier,  $R$ . These results have been obtained integrating numerically the Fokker-Planck equation. The numerical simulations seem to show that the survival

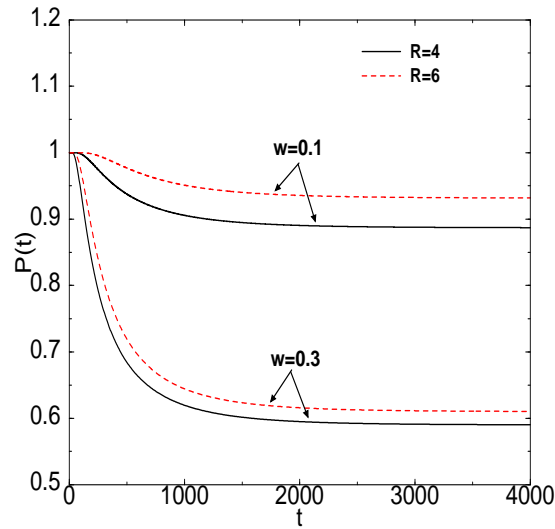


FIG. 4.7. Time evolution of the survival probability  $P(t)$  for two different values of  $R$  and the nonlinearity  $w$ . The parameters are as in Fig. 4.4.

probability tends to stabilize, after a sufficiently long time, at some nonzero (positive) value. Such a value seems to decrease when the nonlinearity becomes stronger (for any given value of  $R$ ), while fewer particles tend to be absorbed when the absorbing boundary is located farther from the initial position of the oscillator, for any given value of  $w$ . In other words, there is numerical evidence that a stronger nonlinearity favors higher absorption of particles, while a farther barrier makes it more difficult. No claim can be made, however, that the survival probability does indeed tend to a nonzero value, when time gets large. In fact, the survival probability might decay so slowly that the numerical simulations cannot fully capture its precise behavior.

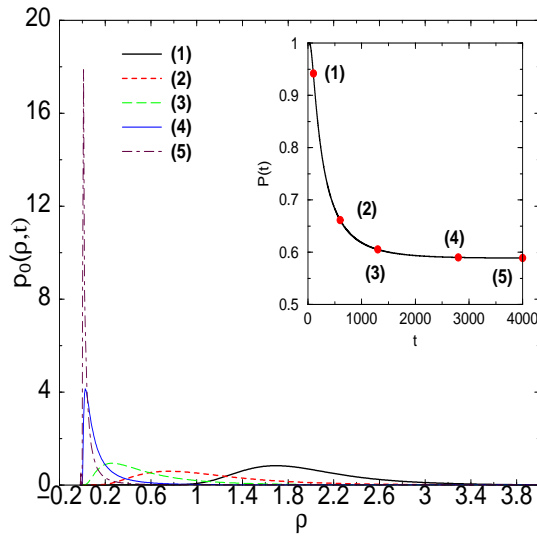


FIG. 4.8. Transition probability density  $p_0(\rho, t)$  versus  $\rho$  for several times. The inset shows the corresponding values of the survival probability for these times. The parameters are as in Fig. 4.4

In Fig. 4.8, the full transition probability density,  $p_0(\rho, t)$ , has been plotted as a function of  $\rho$ , for several times. The inset in this figure shows the corresponding values of the survival probability obtained for the times when the probability density was plotted. This picture illustrates well what happens to the  $\rho$ -profile of  $p_0(\rho, t)$  when time runs. Such profile starts smooth and well spread over the full interval  $0 < \rho < R = 4$ , but as time goes on, it tends to become a Dirac delta function, located at the initial position of the oscillator,  $\rho_0 = 0$ .

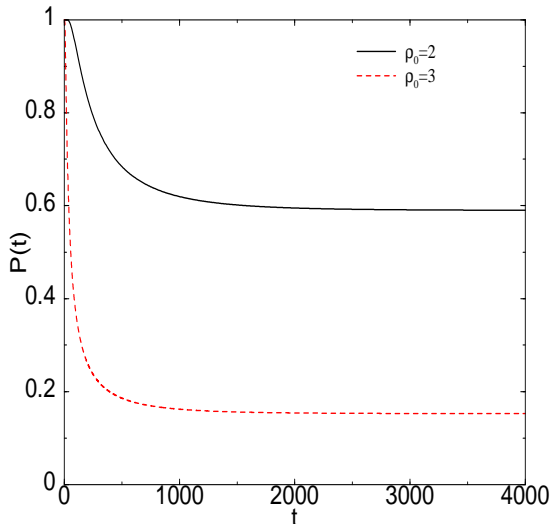


FIG. 4.9. Time evolution of the survival probability  $P(t)$  for two different initial condition data. The parameters are as in Fig. 4.4.

In Fig. 4.9, the dependence of the survival probability on two different initial positions of the oscillator,  $\rho_0 = 2$  or  $\rho_0 = 3$ , is shown. It is clear that the closer such initial position is to the absorbing boundary (located at  $\rho = R = 4$ ), the higher will be the number of the particles absorbed there.

Figure 4.10 displays the dependence of  $p_\infty$  on the nonlinearity parameter,  $w$ . It appears that  $p_\infty$  decreases steadily as  $w$  increases. Here  $R = 4$  was kept fixed. We have also computed the first two moments of the oscillator's displacement,  $y(t)$ , given by (3.9), (3.10). In Fig. 4.11, such moments are shown for the same values of the parameters used in Figs 4.1 and 4.2.

In order to validate the limiting theory, we conducted numerical simulations of the Monte Carlo-type on the stochastic differential equation given in (1.1)-(1.2), with the initial values  $y_\epsilon(0) = \sqrt{2}$ ,  $y'_\epsilon(0) = \sqrt{2}$ . Our purpose was twofold. First of all, we took  $\epsilon$  sufficiently small and  $t$  sufficiently large, to check to what extent it could accurately approximate the original ( $\epsilon$ -labeled process). On the other hand, the numerical results obtained solving the stochastic differential equation have an independent interest, because their validity holds true for any size of  $\epsilon$  and  $t$ . Obviously, whenever  $\epsilon$  is not sufficiently small and/or  $t$  is not sufficiently large, we can expect that the resulting functionals of the limiting process might depart even significantly from those computed on the basis of the stochastic differential equation.

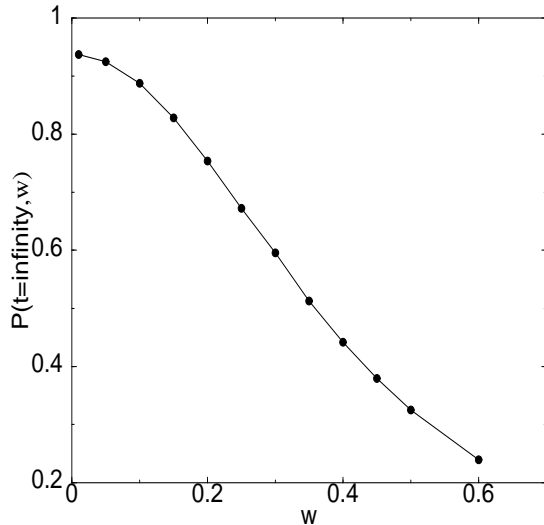


FIG. 4.10. Long-time value of  $p_0(\rho, t)$  obtained in the limit of  $t \rightarrow \infty$  versus the nonlinearity parameter  $w$ . The parameters are as in Fig. 4.4

The Ito-type system can be written as,

$$(4.14) \quad \begin{cases} d\rho = [\epsilon F_1(t; \rho, \varphi; \mu, \nu) + \epsilon^2 G_1(t; \rho, \varphi; \mu, \nu)] dt \\ d\varphi = [\epsilon F_2(t; \rho, \varphi; \mu, \nu) + \epsilon^2 G_2(t; \rho, \varphi; \mu, \nu)] dt \\ d\mu = -\sigma_1 \mu dt + \sigma_1 dW_1 \\ d\nu = -\sigma_2 \nu dt + \sigma_2 dW_2, \end{cases}$$

where we have also displayed the dependence of the functions  $F_i$  and  $G_i$  on the stochastic processes  $\mu$  and  $\nu$ . Since, in the practical simulations, such processes will be colored noise processes with autocorrelations given in (4.1), the system (4.14) includes the last two equations. In fact, according to [11], the colored noise processes above can be evaluated from such Ito equations, driven by the independent standard Brownian motions  $W_1$  and  $W_2$ . The process  $\lambda$  in the damping term is taken to be a constant,  $\lambda(t) \equiv \lambda_0$ .

While the absorbing boundary condition is imposed as a boundary condition on  $\rho = R$  for the Fokker-Planck equation (2.10), here we proceed as follows. Correspondingly to the first time,  $t^*$ , when a given realization  $\rho(t)$  attains the value  $R$ , we ignore the contribution from such realization in the averages yielding the moments of  $\rho$  and  $y$ , for  $t > t^*$ . This procedure yields the moments of the particle position at time  $t$ , taking into account that such a particle did not hit the absorbing barrier yet. Therefore, only the statistical properties of the particles that have survived up to time  $t$  have been included.

In principle, this numerical treatment amounts to a loss of accuracy for larger and larger times, because the sample size (i.e., the number of particles) becomes smaller, thus requiring more realizations when time gets larger. Numerical results, however, show that the fast decay of the moments computed (from the Fokker-Planck equation) is such that the loss of accuracy mentioned above is felt very little.

As usual, the required Monte Carlo simulations can be based on the generation of sequences of (pseudo-) random numbers, which is routine. Here we chose instead to use the so-called sequences of *quasi-random* numbers (deterministic low discrepancy



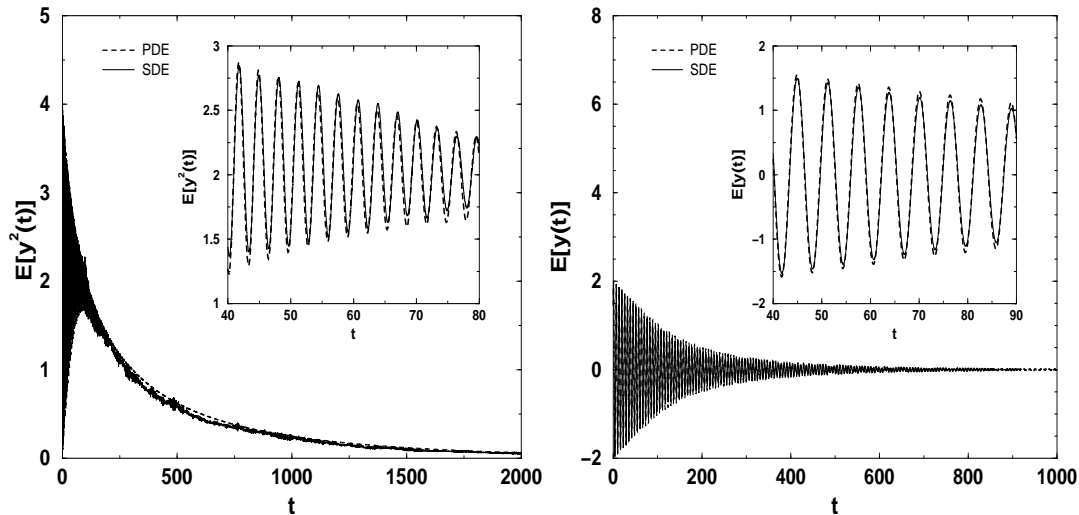


FIG. 4.11. Time evolution of the first and second moment of the oscillator's displacement,  $y$ , keeping  $w$  to the fixed value 0.3. The other parameters are as in Fig. 4.1.

sequences), see [2, 18]. Such a choice provides a higher accuracy for a given number,  $N$ , of realizations, typically involving a deterministic error of order of  $\mathcal{O}(N^{-1} \log^{d^* - 1} N)$  (where  $d^*$  is an “effective dimension”, see [1]), instead of the statistical error of order of  $\mathcal{O}(N^{-1/2})$ . Quasi-random number sequences are rather delicate to exploit, but have been used successfully in a number of applications, see [2, 3, 15, 16, 19]. Application of quasi-random numbers to the numerical solution of stochastic differential equations have been shown to be in general very inefficient, see [10]. In such a paper, however, no “scrambling” strategy was adopted, which action was actually shown to be important in [15, 16]. Here we have implemented a quasi-Monte Carlo algorithm with a reordering technique, as done in [16], and thus our results turned out to be highly accurate. A more general account of a successful implementation of quasi-random sequences to solve stochastic differential equations has been presented in [1].

To solve the system of stochastic differential equations in (4.14), we have implemented a “weak scheme” of order 2 (which reduces to the Heun scheme in the deterministic case), see [14], Ch.15, Sec. 15.1, and [8, 22]. The time-step size used was  $\Delta t = 0.01$ , and  $N = 1000$  realizations. We used Halton sequences of quasi-random numbers [2], being aware that a different choice of them, such as, for instance, Sobol’ or Faure’s numbers, was earlier shown to be essentially irrelevant [17]. In order to simulate random paths to solve the system in (4.14) it is required to generate as many random variables as many time steps, which amounts to generating *high-dimensional* quasi-random sequences. This is a sensible issue, in that high-dimensional quasi-random sequences may fail to work appropriately because unwanted correlations can be easily introduced. Such a difficulty was removed in our algorithm introducing a suitable reordering, as it was done in [16, 15]; see also [1]. Using reordering, the effective dimension of the system reduces to the number of dependent variables,  $\rho$  and  $\varphi$ . Note that the truncation error will be of order  $\mathcal{O}((\Delta t)^2) \approx 10^{-4}$ , which is negligible compared to the quasi-Monte Carlo error, which is of order  $\mathcal{O}(N^{-1} \log N) \approx 0.9 \times 10^{-3}$ .

In Figs 4.1 and 4.2, the continuous line shows the time evolution of the mean

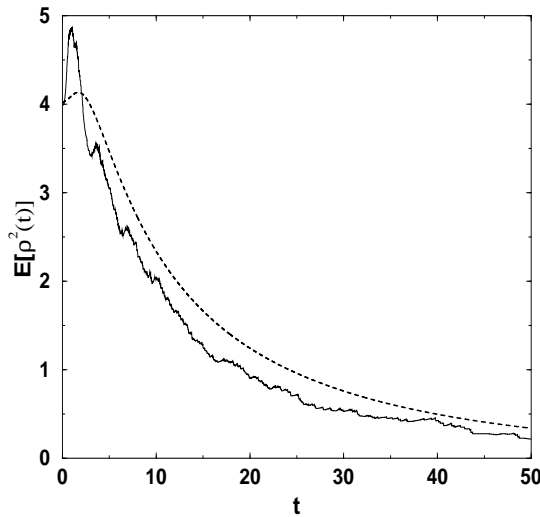


FIG. 4.12. Time evolution of the expected value of  $\rho$ , for  $\epsilon = 0.5$  and  $w = 0.3$ . The other parameters are as in Fig. 4.1

value of the oscillator amplitude,  $\rho$ , of its square,  $\rho^2$ , and the survival probability, with  $\epsilon = 0.1$  and  $w = 0.3$ . Therefore, a comparison is made with the solution obtained in the diffusion limit. The agreement is very good for all times and it also improves when time gets larger in Figs 4.1 and 4.2, being instead a little worse in Fig. 4.4.

In Fig. 4.12, the comparison is made with  $\epsilon = 0.5$ . All these plots show to what extent the diffusion limit provides a good approximation of the original problem in (1.1)-(1.2). In any case, even when  $\epsilon$  is not very small, the qualitative agreement gets better for time sufficiently large. In Fig. 4.11, the mean values of the oscillator's displacement,  $y$ , and of  $y^2$ , are depicted versus  $t$  (solid line). Again, they are compared with the corresponding results obtained through the Fokker-Planck equation (dashed line).

**5. Summary and concluding remarks.** In closing, we stress the high points of the paper. A model for a Duffing oscillator with random parameters and subject to an absorbing boundary condition has been analyzed in the diffusion limit, on a scale where the nonlinear term is much stronger than in the model analyzed in [23]. A higher-order nonlinear effect, such as the appearance of second harmonics effects, can be observed here.

A numerical solution of the stochastic differential equation has been obtained, for small fixed  $\epsilon$ , for both purposes, of validating the diffusion limit theory (when  $\epsilon$  is sufficiently small and  $t$  sufficiently large), and because the problem for finite  $\epsilon$  and  $t$  is meaningful in itself. The dependence on the nonlinearity strength,  $w$ , and on the location,  $R$  of the absorbing boundary has also been investigated, mostly numerically. We have also shown that quasi-random sequences of numbers can be efficiently used in the Monte Carlo simulation, provided that a reordering strategy is adopted.

It is natural to ask whether the problem in (1.1)-(1.2) is meaningful when no absorbing boundary condition is imposed. The (formal) diffusion problem, say  $\mathcal{P}_\infty$ , is described by (2.10)-(2.11) on the unbounded space domain  $(\rho, \varphi) \in (0, +\infty) \times (0, 2\pi)$ . Suppose that we are interested in computing the moments of  $\rho$ , among which the mean

energy  $E[\rho^2]$ . According to (4.12), this requires computing  $p_0(\rho, \tau_1)$ , the solution to equation (3.7) with  $m = 0$ , subject to the initial value  $p_0(\rho, 0) = \delta(\rho - \rho_0)/2\pi$ , on the domain  $0 < \rho < +\infty$ . It turns out that, according to Feller's classification sketched in Section 3, the boundary point  $\rho = +\infty$  is an entrance point. Note that in the model studied in [23] the point  $\rho = +\infty$  was of a different type, namely a natural boundary (as for the heat equation). In [6, 7], it was established that when one of the boundaries is natural while the other is an entrance point, no boundary condition should be imposed (on the latter point), and uniqueness is lost. More precisely, several solutions exist to the problem  $\mathcal{P}_\infty$ , but only one is characterized by being positive and norm-preserving. Therefore, such a solution is a candidate to be a probability density function. Moreover, such a solution enjoys the property of having its value as well as its flux equal to zero at the same time, at  $\rho = +\infty$ , so that this boundary can be considered an absorbing and a reflecting boundary simultaneously. All the other solutions, characterized by an arbitrary value of the flux, are instead either negative or norm-increasing.

In order to compute numerically such a solution,  $p_0(\rho, \tau_1)$ , the problem  $\mathcal{P}_\infty$  has to be approximated by the problem  $\mathcal{P}_{\rho_{\max}}$ , obtained cutting the unbounded domain to the bounded domain  $(0, \rho_{\max})$ . Since the boundary  $\rho = \rho_{\max}$  becomes now regular, a boundary condition can be imposed on it. Recalling that the unique solution to  $\mathcal{P}_\infty$ , i.e., that positive and norm-preserving, vanishes along with its space derivative at  $\rho = +\infty$ , either one of these two conditions at  $\rho = \rho_{\max}$  can be imposed, provided that  $\rho_{\max}$  is sufficiently large. Approximating such a solution to  $\mathcal{P}_\infty$ , (which has an entrance boundary), by the solutions to problems like  $\mathcal{P}_{\rho_{\max}}$ , (which has a regular boundary), is a quite delicate task. In fact, on the one hand a homogeneous Neumann condition is known to preserve the norm of the solution (see equation (2.16)). On the other hand, as it was mentioned before, the solutions to  $\mathcal{P}_\infty$  are very sensitive with respect to small departures from the zero value of the space derivative. Indeed one would obtain either negative or norm increasing solutions. Imposing instead the Dirichlet condition  $p_0(\rho_{\max}, \tau_1) = 0$ , a much more stable behavior would be observed, but the norm of the solution would not be preserved in this case.

## REFERENCES

- [1] Acebrón, J. A., and Spigler, R., *Fast simulations of stochastic dynamical systems*, J. Comput. Phys., **208** (2005), 106-115.
- [2] Caffisch, R. E., *Monte Carlo and quasi-Monte Carlo methods*, Acta Numerica (1998), 1-49 [Cambridge University Press, Cambridge, 1998].
- [3] Caffisch, R.E., Morokoff, W., and Owen, A.B., *Valuation of mortgage-backed securities using Brownian bridges to reduce effective dimension*, J. Comput. Finance, **1** (1997), pp. 27-46.
- [4] Cramér, H., and Leadbetter, M.R., *Stationary and Related Stochastic Processes. (Sample Function Properties and Their Applications)*, Wiley, New York, 1967.
- [5] Di Paola, M., Special Issue of Meccanica, Meccanica, **37** (2002), issue 1-2.
- [6] Feller, W., *Two singular diffusion problems*, Annals Math., **54** (1951), pp. 773-782.
- [7] Feller, W., *The parabolic differential equations and the associated semi-groups of transformations*, Annals Math., **55** (1952), pp. 468-519.
- [8] Higham, D.J., *An algorithmic introduction to numerical simulation of stochastic differential equations*, SIAM Rev., **43** (2001), pp. 525-546.
- [9] Hille, E., *Les Probabilités continues en chaîne*, C.R. Acad. Sci. Paris, **230** (1950), pp. 34-35.
- [10] Hofmann, N., and Mathé, P., *On quasi-Monte Carlo simulation of stochastic differential equations*, Math. Comp., **66** (1997), pp. 573-589.
- [11] Honeycutt, R.L., *Stochastic Runge-Kutta algorithms. II. Colored noise*, Phys. Rev. A, **45** (1992), pp. 604-610.
- [12] Khasminskii, R.Z., *A limit theorem for the solutions of differential equations with a random right hand side*, Theor. Probability Appl., **11** (1966), pp. 390-406.

- [13] Papanicolaou, G., and Keller, J.B., *Stochastic differential equations with applications to random harmonic oscillators and wave propagation in random media*, SIAM J. Appl. Math., **21** (1971), pp. 287–305.
- [14] Kloeden, P.E., and Platen, E., *Numerical Solution of Stochastic Differential Equations*, Springer, Berlin, 1999.
- [15] Lecot, C., and El Khettabi, F., *Quasi-Monte Carlo simulation of diffusion*, J. Complexity, **15** (1999), pp. 342–359.
- [16] Morokoff, W.G., and Cafisch, R.E., *A quasi-Monte Carlo approach to particle simulations of the heat equation*, SIAM J. Numer. Anal., **30** (1993), pp. 1558–1573.
- [17] Morokoff, W.G., and Cafisch, R.E., *Quasi-random sequences and their discrepancies*, SIAM J. Sci. Comput., **15** (1994), pp. 1251–1279.
- [18] Niederreiter, H., *Random Number Generation and Quasi-Monte Carlo Methods*, SIAM, Philadelphia, PA, 1992.
- [19] Ogawa, S., and Lécot, C., *A quasi-random walk method for one-dimensional reaction-diffusion equations*, Math. Computers Simul., **62** (2003), pp. 487–494.
- [20] Papanicolaou, G., *Wave propagation in a one-dimensional random medium*, SIAM J. Appl. Math., **21** (1971), pp. 13–18.
- [21] Papanicolaou, G., and Kohler, W., *Asymptotic theory of mixing stochastic ordinary differential equations*, Comm. Pure Appl. Math., **27** (1974), pp. 641–668.
- [22] Platen, E., *An introduction to numerical methods for stochastic differential equations*, Acta Numerica (1999), 197–246 [Cambridge University Press, Cambridge, 1999]
- [23] Spigler, R., *A stochastic model for nonlinear oscillators of Duffing type*, SIAM J. Appl. Math., **45** (1985), pp. 990–1005.
- [24] Stratonovich, R.L., *Topics in the Theory of Random Noise*, Vols. 1 and 2, Gordon and Breach, New York, 1963.
- [25] Stoker, J.J., *Nonlinear Vibrations in Mechanical and Electrical Systems*, Wiley-Interscience, New York, 1950.
- [26] Yaglom, A.M., *An Introduction to the Theory of Stationary Random Functions*, Englewood Cliffs, N.J., 1962.